Effects of rainfall seasonality and soil moisture capacity on mean annual water balance for Australian catchments

N. J. Potter,[1,2,3] L. Zhang,[1,2] P. C. D. Milly,[4] T. A. McMahon,[2,3] and A. J. Jakeman[5]

Received 30 September 2004; revised 1 March 2005; accepted 10 March 2005; published 9 June 2005.

[1] An important factor controlling catchment-scale water balance is the seasonal variation of climate. The aim of this study is to investigate the effect of the seasonal distributions of water and energy, and their interactions with the soil moisture store, on mean annual water balance in Australia at catchment scales using a stochastic model of soil moisture balance with seasonally varying forcing. The rainfall regime at 262 catchments around Australia was modeled as a Poisson process with the mean storm arrival rate and the mean storm depth varying throughout the year as cosine curves with annual periods. The soil moisture dynamics were represented by use of a single, finite water store having infinite infiltration capacity, and the potential evapotranspiration rate was modeled as an annual cosine curve. The mean annual water budget was calculated numerically using a Monte Carlo simulation. The model predicted that for a given level of climatic aridity the ratio of mean annual evapotranspiration to rainfall was larger where the potential evapotranspiration and rainfall were in phase, that is, in summer-dominant rainfall catchments, than where they were out of phase. The observed mean annual evapotranspiration ratios have opposite results. As a result, estimates of mean annual evapotranspiration from the model compared poorly with observational data. Because the inclusion of seasonally varying forcing alone was not sufficient to explain variability in the mean annual water balance, other catchment properties may play a role. Further analysis showed that the water balance was highly sensitive to the catchment-scale soil moisture capacity. Calibrations of this parameter indicated that infiltration-excess runoff might be an important process, especially for the summer-dominant rainfall catchments; most similar studies have shown that modeling of infiltration-excess runoff is not required at the mean annual timescale.

Citation: Potter, N. J., L. Zhang, P. C. D. Milly, T. A. McMahon, and A. J. Jakeman (2005), Effects of rainfall seasonality and soil moisture capacity on mean annual water balance for Australian catchments, *Water Resour. Res.*, *41*, W06007, doi:10.1029/2004WR003697.

1. Introduction

[2] Catchment-scale water balance is determined by many soil physical, climatic, and ecological factors, and hydrologists aim to gain a better understanding of the interactions of these factors. Models that seek to explain climate-soil-vegetation interactions without relying on streamflow calibration are particularly useful. Furthermore, testing of such models in different climatic and geographical areas is an important part of model evaluation and identification. In this paper, we test the ability of a model slightly modified from that of *Milly* [1994b] to simulate mean annual runoff from Australian catchments.

[3] The primary controls on the mean annual evapotranspiration from a warm region catchment (where snowfall can be disregarded) are rainfall and potential evapotranspiration. Mean annual evapotranspiration cannot exceed the minimum of mean annual rainfall and mean annual potential evapotranspiration. *Budyko* [1974] showed that the ratio of actual evapotranspiration $\overline{ET}$ to rainfall $\overline{P}$ of a catchment is, in general, an increasing function of the aridity, or the dryness index, of the catchment, which is defined as the ratio of mean annual potential evapotranspiration $\overline{E_p}$ to rainfall. Equations describing this function have been proposed in the literature; most of these are empirical [*Zhang et al.*, 2001].

[4] *Budyko* [1974] noted that "systematic deviations" of data points from the empirical curves exist. Budyko identified that the evapotranspiration ratio was likely to be above the empirical curve in catchments where rainfall and potential evapotranspiration occur at the same time in the year. In this paper we investigate this hypothesis that departure from Budyko-like empirical curves can be explained by differences in the seasonal timing of rainfall. Such a sensitivity of water balance to seasonality of climate is consistent with Milly's supply-demand-storage model [*Milly*, 1994a, 1994b].

[1] CSIRO Land and Water, Canberra, ACT, Australia.
[2] Cooperative Research Centre for Catchment Hydrology, Clayton, Victoria, Australia.
[3] Department of Civil and Environmental Engineering, University of Melbourne, Melbourne, Victoria, Australia.
[4] U.S. Geological Survey, Princeton, New Jersey, USA.
[5] Integrated Catchment Assessment and Management Centre and Centre for Resource and Environmental Studies, Australian National University, Canberra, ACT, Australia.

0043-1397/05/2004WR003697$09.00

[5] Many stochastic soil moisture models [*Milly*, 1993; *Rodriguez-Iturbe et al.*, 1999; *Laio et al.*, 2001] explore the effects that the random variability of rainfall depths and arrival times has on the mean annual water balance. *Woods* [2003] developed a related water balance model with more extensive process descriptions, particularly canopy and saturated zone submodels. *Milly* [1994a] investigated how the seasonal changes in water supply and demand of a catchment affect the mean annual water balance. *Milly* [1993, 1994a] found that neither random nor seasonal variation alone was sufficient to explain the mean annual water balance and that both types of variation generally contributed to the overall balance.

[6] *Milly* [1994b] proposed a catchment-scale soil moisture accounting model, which represents precipitation and potential evapotranspiration inputs as seasonally varying functions, and tested the model for the part of the United States east of the Rocky Mountains by combining precipitation, runoff and soil moisture capacity estimates on a grid with 0.5° spatial resolution. He found that "the agreement between model and observations in the present study supports the assumptions underlying the theory"; those assumptions include the neglect of infiltration-excess runoff.

[7] Many studies have shown that relatively simple models can be successful in explaining the water balance of catchments in the United States [*Milly*, 1994b; *Wolock and McCabe*, 1999; *Sankarasubramanian and Vogel*, 2002], New Zealand [*Atkinson et al.*, 2002], and Australia [*Farmer et al.*, 2003] at mean annual scale. Greater detail is required in modeling hydrological processes at smaller timescales, but none of these papers modeled infiltration-excess runoff in explaining mean annual water balance.

[8] Stochastic soil moisture models, such as the ones cited above, are useful for exploring controls on mean annual water balance, because they allow an explicit quantification, sometimes with analytical solutions, of the effect that different timescales of variability in water and energy supply have on the mean annual water balance. These models also require relatively few parameters, as compared to other models, and no calibration with streamflow records. For these reasons, and also in order to further test Milly's model, we chose to use a slightly modified version of *Milly*'s [1994b] model to explain the mean annual water balance of a number of Australian catchments.

[9] Section 2 describes the modeling framework and data used in this study. Solutions are discussed in section 3. In section 4, catchments are categorized with respect to rainfall seasonality, and evapotranspiration is analyzed by category without model calibration. Soil moisture capacities are then calibrated for each catchment and the calibrated values are compared with the a priori (uncalibrated) values. The results of section 4 are discussed in section 5.

2. Modeling Approach

2.1. Data Used

2.1.1. Rainfall and Runoff Data

[10] The rainfall and runoff data used in this study were obtained from the data set described by *Peel et al.* [2000]. These data consist of daily, catchment-averaged rainfall totals and monthly unimpaired streamflow totals at 331 gauging stations around Australia. Gridded rainfall data were provided by the Queensland Department of Natural Resources and Mines, based on interpolation of over 6000 rainfall stations in Australia; this gridded data were then averaged over each catchment. Further details can be found in [*Peel et al.*, 2000]. Although *Peel et al.* [2000] extended the streamflow records by applying a rainfall-runoff model to the data, we used only the observed streamflow data. The catchments range in size from 50 to 2000 km^2.

[11] The mean annual rainfall and runoff were computed from monthly totals. All catchments in the data set were required to have at least 120 months of precipitation and streamflow data, although these months were not required to be contiguous. Although, in general, the rainfall records were longer than the streamflow records, we used only months with recorded streamflow data to calculate the parameters for the rainfall data. This was done to ensure that the rainfall data were consistent with the runoff data. "Observed" evapotranspiration in a catchment was taken to be the difference between observed rainfall and runoff.

2.1.2. Soil Moisture Capacity Estimates

[12] We used estimates of plant-available water capacity from *McKenzie et al.* [2003]; these estimates were obtained by integration of profile available water capacity over plant-dependent root depth distributions. The soil depth was estimated using terrain analysis in conjunction with conventional sources of soil information. Profile available water capacity was determined by pedotransfer functions or water retention measurements in the catchment; notional field capacity and wilting point were defined at matric potentials of −10 kPa and −1.5 MPa. Because our model was configured for most of the analyses as a spatially lumped model, spatially averaged values of the plant-available water capacity of *McKenzie et al.* [2003] were used to obtain the catchment-scale soil moisture capacity s_{max} in our model. In a sensitivity analysis testing the effect of spatial variability, we used an arbitrary parameterization to define variability around the mean.

[13] *Ladson et al.* [2004] estimated soil moisture capacity for 180 catchments around Australia using an empirical approach: soil moisture data were collected from previous studies; soil moisture capacity was defined as the difference between the wettest and driest observations. We used these data as an independent check on the implication, from model calibration, of a systematic dependence of the soil moisture capacities on the seasonality categorization of the catchments.

2.1.3. Potential Evapotranspiration Values

[14] Mean monthly areal potential evapotranspiration was calculated by use of the Priestley-Taylor equation [*Priestley and Taylor*, 1972]. The input data (derived solar radiation, temperature and humidity) were produced by the Australian Commonwealth Bureau of Meteorology and were subsequently interpolated and gridded by the Queensland Department of Natural Resources and Mines. The spatial resolution of the data is 0.05°, and the data cover the period 1980–1999. Mean monthly values of potential evapotranspiration for each catchment were calculated from gridded potential evapotranspiration values [*Raupach et al.*, 2001a]; these grids were averaged over the catchment areas. Further details are given by *Raupach et al.* [2001a, 2001b].

Table 1. Summary Statistics of Catchment Areas, Percentage Forest Cover Estimate, Average Rainfall Intensity, Maximum Altitude Within the Catchment Minus Average Altitude of the Catchment, and Average Soil Permeability[a]

	Area, km^2	Percent Forest Cover	Average 30-min Rainfall Depth, mm	Maximum Minus Average Altitude, m	Average Soil Permeability, mm hr^{-1}
			All Catchments		
Mean	417	54	8.47	471	135.6
SD	377	30	1.59	260	81.0
Median	296	54	8.38	412	104.2
			Summer		
Mean	413	57	9.89	500	143.6
SD	408	28	1.18	242	80.2
Median	293	64	9.79	429	121.2
			Nonseasonal		
Mean	417	53	8.31	476	116.0
SD	366	31	0.72	223	74.4
Median	312	48	8.28	444	100.0
			Winter		
Mean	423	51	6.91	433	141.4
SD	354	32	0.99	303	85.1
Median	304	53	6.95	341	108.3

[a]Note that rainfall intensity data were only available for 224 of the catchments.

[15] We also used independently estimated values of areal potential evapotranspiration obtained from the *Bureau of Meteorology* [2001] for comparison. These estimates are based on Morton's complementarity relationship, and provided an independent way of ensuring the accuracy of the potential evapotranspiration estimates from *Raupach et al.* [2001a].

[16] In total, we were able to study 262 catchments across Australia. This was the number of catchments with adequate rainfall, runoff, soil moisture capacity and potential evapotranspiration data.

2.1.4. Other Data

[17] Some summary statistics for the catchments studied are shown in Table 1. These statistics are presented for all catchments, and separated into the rainfall seasonality categories defined in section 4.1. The data summarized in Table 1 are not used directly in the model described in section 2.3.

[18] Values of average 30-min rainfall depth for each catchment were estimated by calculating the value of *Lu et al.*'s [2003, Figure 21] estimated 30-min rainfall depth at the site of the gauging station of each catchment. *Lu et al.*'s [2003] rainfall intensities are only provided between latitudes 24°S and 40°S and longitudes 154°E to 136.25°E. Nevertheless, 224 of the 262 catchments lie within this area.

[19] The soil permeability estimates are values of saturated hydraulic conductivity in the A horizon, taken from the Atlas of Australian Soils [*McKenzie et al.*, 2000]. These values were averaged across the catchment polygons.

2.2. Fu's Curve

[20] A number of empirical curves have been developed to interpolate mean annual evapotranspiration data, such as the data in Figure 1. For example, *Budyko* [1974, pp. 324–325] defines several empirical curves and notes "The choice of one or another interpolation function...is not very important," as any number of functions have the same general shape. One particular curve, developed by Fu and explained in detail by *Zhang et al.* [2004], is derived as the solution to a set of differential equations that represent physically meaningful boundary conditions and conditions on the derivatives of an interpolating function:

$$\frac{\overline{ET}}{\overline{P}} = 1 + \frac{\overline{E_p}}{\overline{P}} - \left[1 + \left(\frac{\overline{E_p}}{\overline{P}}\right)^{\alpha}\right]^{1/\alpha}. \quad (1)$$

Here α is a fitting parameter. Increasing α gives higher values of the evapotranspiration ratio for a given dryness index. This result makes Fu's curve a flexible tool for modeling evapotranspiration ratios. We used Fu's curve to quantify the average relationship of the evapotranspiration ratio to the dryness index for different seasonality categories (Figure 1).

2.3. Model

[21] In order to estimate the mean annual water balance at catchment scale, we used a lumped, explicit soil moisture accounting model. Rainfall was represented as a seasonally varying Poisson white noise process, and potential evapotranspiration was represented as a seasonally varying constant.

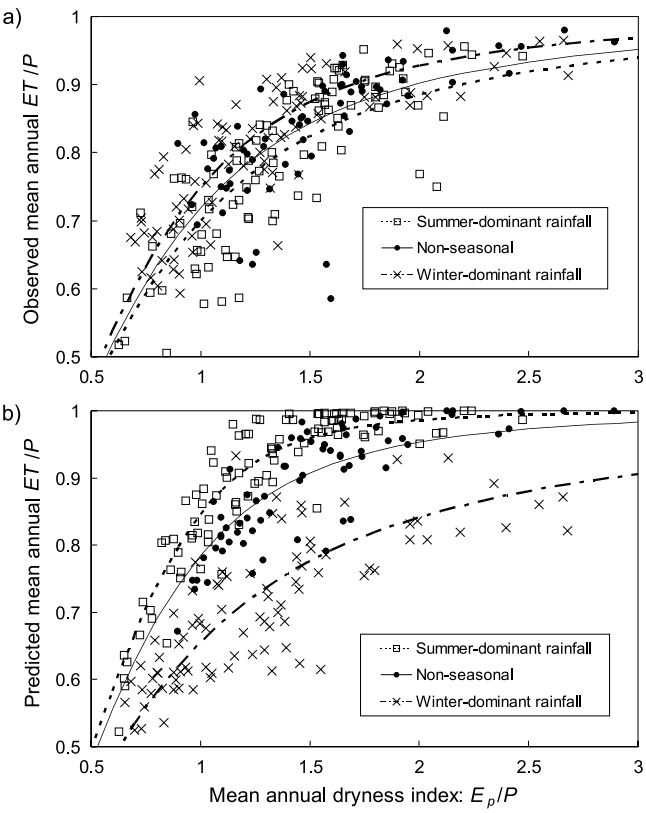

Figure 1. (a) Observed and (b) predicted mean annual evapotranspiration ratios as a function of the dryness index. The least squares Fu curves fitting these points are plotted for each seasonality category. The Fu curves interpolating all the ratios have been omitted for clarity.

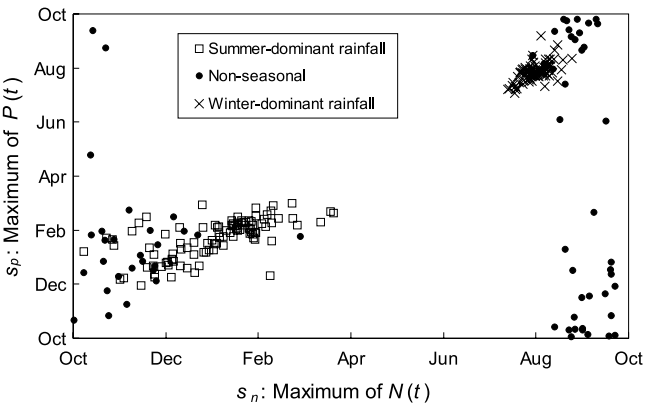

Figure 2. Categorization of catchment rainfall regimes. Seasonal and nonseasonal categorizations were made according to the size of δ_p parameters from equation (3), whereas the determination of seasonality was made by the natural grouping of s_n and s_p, the times at which equations (2) and (3) are maximized. Since the δ_p parameters are smaller for the nonseasonal catchments, the values of s_n and s_p for these catchments are less well defined. However, the nonseasonal points lie mostly between the winter and summer-dominant rainfall points.

[22] The soil moisture content of the catchment can be modeled as a single, representative store. Alternatively, the spatial variation of soils and vegetation can be modeled by assuming a gamma distribution of soil moisture capacities across the catchment. The soil is assumed not to limit the infiltration rate. Any storage of water in excess of field capacity is rapidly removed from the moisture store by gravity, and is assumed eventually to pass through the groundwater system and become runoff. The rapid drainage simplification is warranted because the timescale of root zone drainage is much shorter than that of interstorm evapotranspiration. We are not concerned with the subsequent subsurface movement or storage of this water in the groundwater system, because our analyses address only long-term mean runoff. The motivation for choosing this model is that the soil and vegetation characteristics of the catchment can be described and modeled relatively simply. The climate (for which we generally have more reliable data, as compared with soil and vegetation data) is modeled in more detail.

[23] Thus the formulation of the model is identical to the model of *Milly* [1994b], with one minor difference. The curves describing the climate forcing can have extrema at arbitrary times during the year. Milly's model assumes, as a first-order approximation, that the extrema (either maximum or minimum) of all the curves must occur at the same time in the year. We generalized this approximation to allow more flexibility in the modeling of seasonality. Whereas the timing of the maximum of potential evapotranspiration was generally constant across all the catchments, Figure 2 shows that the data have a broad range in timing of maxima of rainfall.

[24] Adding arbitrary phase shifts to the three climate curves introduced only marginal complexity to the solutions (see section 3.1) and is justified by the wide range of rainfall phase shift parameters that we obtained from fitting the data. We found no justification for using a higher-order Fourier function instead of a cosine function.

2.3.1. Rainfall and Runoff Processes

[25] The rainfall arrival process is modeled as a periodic generalization of a Poisson process. Whereas a standard Poisson process has a constant expected arrival rate, the generalization we use has a periodic expected rate $N(t)$. The number of storms arriving during the time period $(0, t)$ is distributed as a Poisson random variable with mean equal to $\int_0^t N(\tau)d\tau$. We modeled the rainfall arrival rate $N(t)$ as a cosine curve:

$$N(t) = \overline{N_d}[1 + \delta_n \cos\omega(t - s_n)], \tag{2}$$

where $\overline{N_d}$ is the average daily storm arrival rate. The nonnegative parameter δ_n is the amplitude of the daily rainfall arrival rate curve relative to the average daily rate $\overline{N_d}$. The choice of a cosine function, as opposed to a sine function, means that if $\delta_n > 0$, s_n has the simple interpretation of being the time of the year at which $N(t)$ is at a maximum. The scaling factor $\omega = 2\pi/365$ means that the s_n parameter is measured in days rather than radians.

[26] The mean daily rainfall rate is also modeled as a cosine curve:

$$P(t) = \overline{P_d}\left[1 + \delta_p \cos\omega\left(t - s_p\right)\right]. \tag{3}$$

$\overline{P_d}$ is an average daily rate and the parameters δ_p and s_p have interpretations analogous to those of δ_n and s_n. The integral of $P(t)$ over one day is the mean daily rainfall for that particular day in the year. The depth of a storm is modeled as an independent exponential random variable with mean $P(t)/N(t)$.

[27] As already noted, infiltration-excess runoff is not included in the model. Infiltration-excess runoff is more difficult to model than the storage-excess runoff considered here, because it depends also on rainfall intensity as well as soil permeability, and would thus require an additional variate in the rainfall model. We expect that if infiltration-excess runoff is a major runoff generation process, the current modeling approach will be unsatisfactory.

2.3.2. Evapotranspiration Process

[28] The potential evapotranspiration rate is assumed to be a cosine curve, with annual period, given by the parameterization

$$E_p(t) = \overline{E_{pd}}[1 + \delta_e \cos\omega(t - s_e)], \tag{4}$$

with $\overline{E_{pd}}$ equal to the average daily rate of potential evapotranspiration and the other variables similar to those in equations (2) and (3). That is, the rate of potential evapotranspiration is a time-dependent, but nonrandom, variable. In our model and the models of *Milly* [1993, 1994a, 1994b], the ratio of actual to potential evapotranspiration is a step function of soil moisture at any time; actual evapotranspiration occurs at the (time-dependent) potential rate whenever the soil moisture is greater than the wilting point, and is zero otherwise. The rate of actual evapotranspiration is assumed in other models to vary linearly with soil moisture at low levels of soil moisture. *Milly* [2001] provides a justification for using the simpler

step function rather than the more complex "ramp" function. Milly notes according to the models of *Milly* [1993] and *Rodriguez-Iturbe et al.* [1999] that "the partitioning of precipitation into runoff and evapotranspiration by the two models is compared . . . Differences are very small." The soil moisture probability density function derived from *Milly*'s [1993] model is found to be in close accordance with Rodriguez-Iturbe's, especially for humid catchments with dryness index less than 1; Milly noted that the difference was greatest for arid catchments. This is because the soil moisture content is more likely to be at or below the threshold level in arid catchments than in humid catchments. The difference between ramp and step functions is discussed in more detail in section 5.3.

2.3.3. Spatial Variability of the Catchment Soil Moisture Capacity

[29] *Milly* [1994b] assumed that the soil moisture capacity of a catchment follows a gamma distribution with parameters λ and κ. The mean of the distribution, λ, is the catchment-scale soil moisture capacity estimate s_{max}, whereas the coefficient of variation of the distribution is equal to $\kappa^{-1/2}$.

[30] *Milly* [1994b] showed that if the catchment-scale soil moisture capacity is spatially variable over a catchment, then the predictions of mean annual evapotranspiration will be smaller than predictions in the absence of spatial variability. We allowed the soil moisture capacity to vary spatially according to *Milly*'s [1994b] assumption, with values for the κ parameter of 2, 1, and 1/2. Results were consistent with Milly's: smaller values of κ resulted in lower evapotranspiration ratios (and hence lower Fu curves and α values) for each seasonality category. These results are not included.

[31] As is shown later, we found that the differences between the observed and predicted evapotranspiration ratios varied systematically with the seasonality categories characterizing catchments. In calculations not described here, we found that the consideration of spatial variability did not explain this systematic difference. Consistent with a "top-down" modeling approach, we did not include spatial variability of s_{max} parameter. As such, the results in the remainder of this study were all calculated by assuming that the s_{max} parameter is constant across each catchment.

2.4. Estimation of Model Parameters

[32] The model described above requires 10 parameters: the catchment-scale soil moisture capacity s_{max}, and three parameters for each of the equations (2), (3) and (4). The three parameters required in the daily rainfall curve (3) were estimated by finding the parameters that minimize the sum of the squared difference between the daily rainfall curve and the mean daily rainfall amounts. The three parameters required for equation (4) were fitted in the same manner to the monthly potential evapotranspiration values.

[33] We used the method of moments to estimate the average rainfall arrival rates, as described by *Rodriguez-Iturbe et al.* [1984]. The mean and variance were based on daily rainfall totals. That is, let P_i be the average rainfall, and N_i the expected number of rainfall events for the ith day of the year. Then from equations (7) and (8) of *Rodriguez-Iturbe et al.* [1984], and with the assumption that rainfall depths are exponentially distributed, the method-of-moments estimate for N_i can be calculated as

$$N_i = \frac{2[E(P_i)]^2}{Var(P_i)}, \tag{5}$$

where the expectation ($E(\cdot)$) and variance ($Var(\cdot)$) in the equation are sample moments of the rainfall record. The parameters of the seasonal rainfall rate curve, equation (2), can then be estimated by applying the least squares procedure to these method-of-moments estimates of the mean number of storms per day, N_i.

3. Solving for Mean Annual Evapotranspiration

3.1. Analytical Solutions for Special Cases

[34] The general solution for the mean annual evapotranspiration ratio must be obtained by numerical methods. However, *Milly* [1994b] derived analytical solutions for the mean annual evapotranspiration ratio for three special cases: the absence of temporal variability of rainfall and potential evaporation; the absence of a seasonal cycle; and infinite storm arrival rate, or a continuous rainfall rate. The first two of these are applicable to the modified model presented here. The third [*Milly*, 1994b, equations (22)–(23)] (as well as the numerical solution) needs a slight modification to accommodate the extra parameters s_n, s_p and s_e.

3.2. Numerical Solution for the General Case

[35] An analytical solution for the expected value of annual evapotranspiration for the general problem presented above has not been found. However, mean annual evapotranspiration can be computed numerically by Monte Carlo simulation [*Milly*, 1994b]. We used this approach to compute the results presented in this paper. Convergence of the simulated mean annual evapotranspiration was obtained to within less than 1% after running the simulations for 50,000 years.

[36] Some of the catchments, in particular those in northern Queensland and Western Australia, had strongly seasonal rainfall regimes, with very low average daily rainfall during the dry season. The δ_p parameter of eight of these catchments was greater than one. In these cases, we constrained the rainfall rate curve (3) to be positive within the Monte Carlo simulation. This resulted in a modeled mean annual rainfall bias on the order of 2–3% in some of these catchments. We considered either using a periodic function with subannual harmonics for some of these catchments, and leaving them out of the study altogether. However, there were only a small number of highly seasonal catchments in the study; and none of these have true wet and dry seasons with zero rainfall rate in the dry season.

4. Results

4.1. Rainfall Seasonality

[37] In an analysis of the harmonics of the Fourier transform of both the average daily rainfall rate and the average storm arrival rate, we found that only the annual harmonic was justified. The magnitudes of the subannual harmonics were comparable to those due to random variability. Thus the modeled rainfall rates, equations (2) and

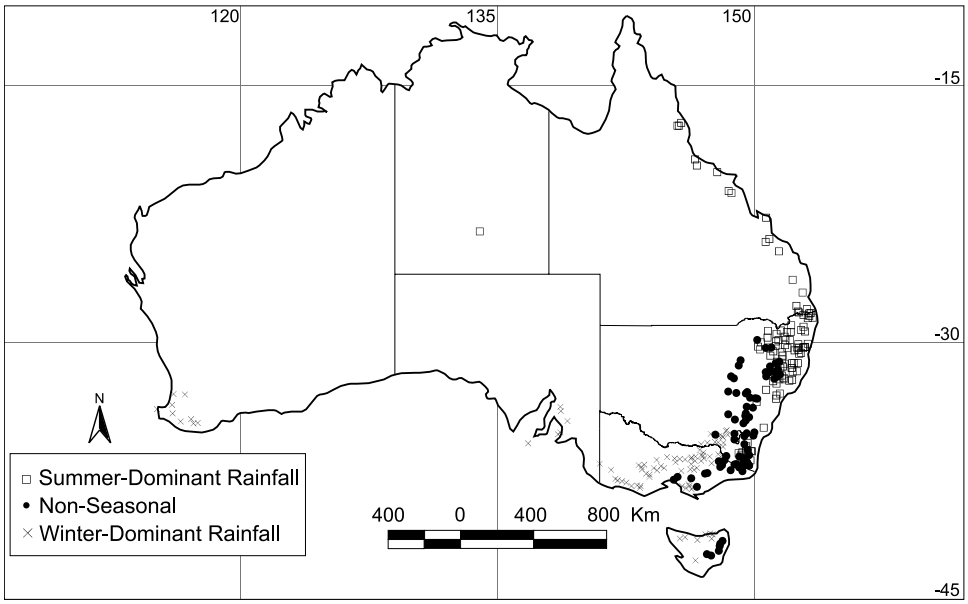

Figure 3. Geographical distribution of rainfall regimes. The categorization into catchment rainfall seasonalities, as described in section 4.1 and shown in Figure 2, also results in a clear geographical spread of catchment categories.

(3), describe the average rainfall regime at each catchment well.

[38] Strictly speaking, catchment seasonality should be defined by both the potential evapotranspiration and rainfall. However, because of the large spatial coherence in seasonality of potential evapotranspiration over the study region (90% of the s_e parameters were in a 14.5-day range), we opted to define seasonality instead simply in terms of rainfall.

[39] The rainfall regimes were determined by examining Figure 2. Catchments with nonseasonal rainfall regimes were defined as those with small seasonal rainfall amplitudes (δ_p less than 0.25). The remainder of the catchments were then grouped into summer- and winter-dominant rainfall catchments by the value of the s_p and s_n parameters. As can be seen from Figure 2, there is a clear distinction between summer- and winter-dominant rainfall catchments when δ_p is greater than 0.25. The choice of the 0.25 threshold was arbitrary. The number of catchments belonging to each seasonality category were as follows: 103 catchments were categorized as having summer-dominant rainfall, 69 as nonseasonal, and 90 as having winter-dominant rainfall regimes.

[40] The summer-dominant rainfall catchments are mostly located north of latitude 30°S, with some additional catchments south of this on the coast, and at Alice Springs in the center of Australia (Figure 3). Winter-dominant rainfall catchments are mostly located in the state of Victoria, south of latitude 35°S, in South Australia and in Western Australia, with some in Tasmania. The nonseasonal catchments are located between the two areas of winter- and summer-dominant rainfall on the southeastern coast of Australia.

[41] The alternative [*Ladson et al.*, 2004] soil moisture capacity estimates were taken from different catchments to the *McKenzie et al.* [2003] estimates. We assigned the rainfall seasonality of the closest catchment in the main data set to each catchment in the *Ladson et al.* [2004] data set. Because the seasonality categories have a clear geographical pattern, this procedure is reasonable. Ninety of the catchments from *Ladson et al.* [2004] were classified as summer-dominant, 23 were classified as nonseasonal, and 67 were classified as winter-dominant. The *Ladson et al.* [2004] soil moisture capacity estimates were not used directly for modeling. We used these independently estimated capacities for comparison only.

4.2. Effect of Seasonality on Evapotranspiration Ratios

[42] Figure 1 shows the observed and predicted evapotranspiration ratios versus the dryness index for each catchment. Data for all of the catchments are shown, except for the catchment near Alice Springs, which has an extreme surplus of potential evapotranspiration over rainfall with a dryness index of about 7. For both observed and predicted values, we interpolated Fu curves through all the evapotranspiration ratios and for each seasonality category. Figure 1 displays the Fu curves for each seasonality category, but not the overall Fu curves. The corresponding α values for these eight curves are shown in Table 2. For the observed mean annual evapotranspiration ratios, the summer-dominant rainfall curve lies below the winter-dominant rainfall curve, whereas for the predicted ratios, the summer-dominant rainfall curve is above the winter-dominant rainfall curve.

[43] In order to test whether the seasonal dependence of these curves was statistically significant, we calculated (for each seasonality category) the difference between the mean annual evapotranspiration ratios and the Fu curves that interpolate all the ratios. The mean, standard errors and t statistics for each of these sets of residuals are displayed in Table 3. If there were no significant difference between the evapotranspiration ratios for each seasonality category, the t statistics would be small.

[44] The t statistics for the summer-dominant rainfall and winter-dominant rainfall catchment residuals are greater than

Table 2. Values of Fu's α Parameter for the Different Seasonal Categories[a]

	Observed $\overline{ET}/\overline{P}$	Predicted $\overline{ET}/\overline{P}$
All Catchments	2.82	3.25
Summer	2.64	4.84
Nonseasonal	2.80	3.55
Winter	3.10	2.35

[a]These are the parameters used in equation (1) for the curves in Figure 1, which give the least squares fit to the data.

the two-sided 95% critical values of ±1.96 (using a normal approximation) for both observed and predicted evapotranspiration ratios. This result confirms that the observed evapotranspiration values for the summer-dominant rainfall catchments are significantly below the average Fu curve, whereas the observed evapotranspiration values for the winter-dominant rainfall catchments lie above the average curve; the opposite is true for the predicted values.

4.3. Comparison of Predicted Evapotranspiration With Observed Values

[45] Figure 4 shows observed mean annual evapotranspiration versus predicted mean annual evapotranspiration. Superimposed over this plot is a 1:1 line for comparison. The coefficients of linear regressions for each seasonality category and the corresponding R^2 values are displayed in Table 4.

[46] In order to compare the observed and predicted evapotranspiration ratios for each seasonality category, we calculated the difference between the observed evapotranspiration ratios and the Fu curves interpolating the predicted evapotranspiration ratios. By performing t tests on the means of these residuals, we can determine whether the observed and predicted evapotranspiration ratios, for each seasonality category, differ significantly. This also allows us to gain some idea whether the α parameters in Table 2 are statistically different for the observed and predicted cases. The t tests for these values are displayed in Table 5.

[47] The t statistic for all of the catchments as a group is significantly different from zero. This difference indicates that overall, the model significantly overpredicts mean annual evapotranspiration. This overprediction is confirmed by the regressions slopes of the lines through the origin in Table 4. The t statistic in Table 5 for the winter-dominant rainfall catchments is significantly positive, which means that the Fu curve interpolating the predicted evapotranspiration ratios for the winter-dominant rainfall catchments is lower than the observed evapotranspiration ratios. Conversely, evapotranspiration in the summer-dominant rainfall and nonseasonal rainfall catchments is significantly overpredicted.

4.4. Calibration of Soil Moisture Capacities

[48] Recall that the estimates of the catchment-scale soil moisture capacities of *McKenzie et al.* [2003] have been obtained independently from the present study. This parameter is critical to the water balance predictions, because soil moisture storage is a buffer between the seasonal supply and demand of moisture from the catchment. In order to test the current modeling approach, and to gain insight into the estimates of *McKenzie et al.* [2003], we calibrated soil moisture capacities for each catchment so that the predicted mean annual evapotranspiration would be equal to the observed.

[49] These calibrated soil moisture capacities are shown in a histogram in Figure 5b. Compared with the soil moisture capacities from *McKenzie et al.* [2003] (Figure 5a), the calibrated soil moisture capacities for catchments with summer-dominant rainfall are extremely low. Many of the nonseasonal catchments also have low calibrated capacities. The calibrated capacities for the winter-dominant rainfall catchments, in contrast, are generally larger than the capacities from *McKenzie et al.* [2003].

[50] The calibrated soil moisture capacities are plotted against the soil moisture capacities from *McKenzie et al.* [2003] in Figure 6. Regression lines were calculated for each of the seasonality categories, and the regression coefficients are presented in Table 6. Overall, the calibrated values and the estimated values are not very similar. Figure 6 shows that there are large differences between the two in some instances, especially for the winter-dominant catchments.

5. Discussion

[51] The results, as shown in Figure 1 and Table 2, demonstrate that for a given mean annual climate, the model predicts that more rainfall is evapotranspired in those catchments with summer-dominant rainfall than in those with nonseasonal or winter-dominant rainfall. The data indicate that the opposite is true of the observed evapotranspiration ratios; that is, evapotranspiration ratios are more likely to be higher in winter-dominant rainfall catchments than in others. The t statistics from Table 3 demonstrate this statistically. The linear regressions of the predicted mean annual evapotranspiration against the observed mean annual evapotranspiration (Table 4 and Figure 4) also confirm this analysis. The predictions for winter-dominant rainfall catch-

Table 3. Residuals From the Fu Curve Interpolating All $\overline{ET}/\overline{P}$ Ratios for Both Observed and Predicted Values[a]

		Observed $\overline{ET}/\overline{P}$ – Overall Fu Curve For Observations			Predicated $\overline{ET}/\overline{P}$ – Overall Fu Curve for Predictions		
	Number of Catchments	Mean × 100	Standard Error × 100	t Statistic	Mean × 100	Standard Error × 100	t Statistic
All	262	0.00	0.47	0.0	−0.04	0.56	−0.1
Summer	103	−2.19	0.76	−2.9	7.00	0.42	16.9
Nonseasonal	69	−0.08	0.95	−0.1	2.21	0.55	4.0
Winter	90	2.58	0.67	3.9	−9.83	0.72	−13.6

[a]Observed values are shown in Figure 1a, and predicted values are shown in Figure 1b. The mean and standard error of these residuals have been multiplied by 100 for clarity.

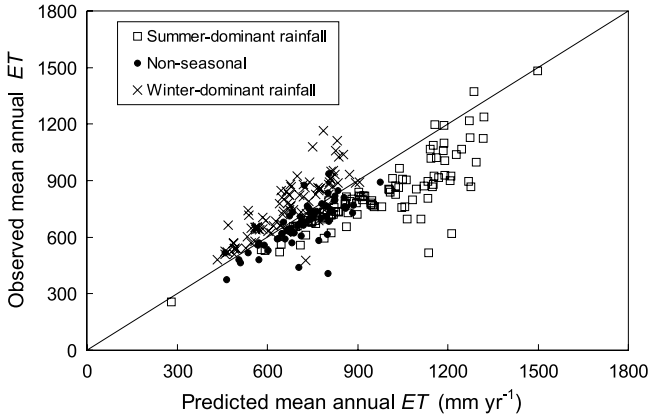

Figure 4. Observed mean annual evapotranspiration plotted versus modeled predictions. The 1:1 line is plotted for comparison.

ments are lower than for the summer-dominant rainfall catchments, whereas the mean annual evapotranspiration is overpredicted in summer-dominant rainfall catchments. Overall, the summer-dominant rainfall catchments tend to affect the regression line for all of the catchments.

5.1. Calibrated Catchment-Scale Soil Moisture Capacities

[52] Table 6 contains the coefficients for the regressions of calibrated soil moisture capacities versus the values estimated by *McKenzie et al.* [2003]. The calibrated and estimated soil moisture capacities are poorly correlated for all the seasonality categories. Figures 5 and 6 show that the calibrated values of s_{max} for winter-dominant rainfall catchments exhibit a wide spread and are very much larger than the estimated values. Furthermore, even the intercept of the regression in Table 6 for winter-dominant rainfall catchments is larger than the majority of estimated s_{max} parameters for all of the catchments analyzed in this study, as shown by Figure 5.

[53] The average values of the calibrated soil moisture capacities were 28.5 mm for the summer-dominant rainfall catchments, 56.0 mm for the nonseasonal rainfall catchments, and 199.2 mm for the winter-dominant rainfall catchments. The catchments with summer-dominant rainfall

Table 4. Coefficients and R^2 Values of the Regressions of Mean Annual Evapotranspiration[a]

	R^2	Slope	Slope 95% Confidence Interval	Intercept	Intercept 95% Confidence Interval
Linear Regression of Predictions					
All	0.56	0.61	(0.54, 0.67)	271	(217, 326)
Summer	0.69	0.75	(0.65, 0.85)	92	(−5, 188)
Nonseasonal	0.57	0.84	(0.67, 1.01)	67	(−59, 193)
Winter	0.67	1.04	(0.89, 1.19)	57	(−47, 161)
Regression of Predictions Through the Origin					
All	0.39	0.93	(0.91, 0.95)		
Summer	0.68	0.84	(0.82, 0.86)		
Nonseasonal	0.57	0.93	(0.91, 0.95)		
Winter	0.67	1.12	(1.10, 1.15)		

[a]Regressions were performed on the data in Figure 4 (observed mean annual evapotranspiration against predicted evapotranspiration).

Table 5. Residuals of the Observed $\overline{ET}/\overline{P}$ Ratios From the Predicted Fu Curves for Each Seasonality Category[a]

	Number of Catchments	Observed $\overline{ET}/\overline{P}$ − Predicted $\overline{ET}/\overline{P}$ From Seasonal Fu Curves: Mean × 100	Standard Error × 100	t Statistic
All	262	−3.8	0.47	−8.1
Summer	103	−13.0	0.79	−16.4
Nonseasonal	69	−6.0	1.02	−5.9
Winter	90	8.9	0.68	13.1

[a]These residuals are the $\overline{ET}/\overline{P}$ ratios from Figure 1a minus the Fu curves in Figure 1b. The mean and standard error of these residuals have been multiplied by 100 for clarity.

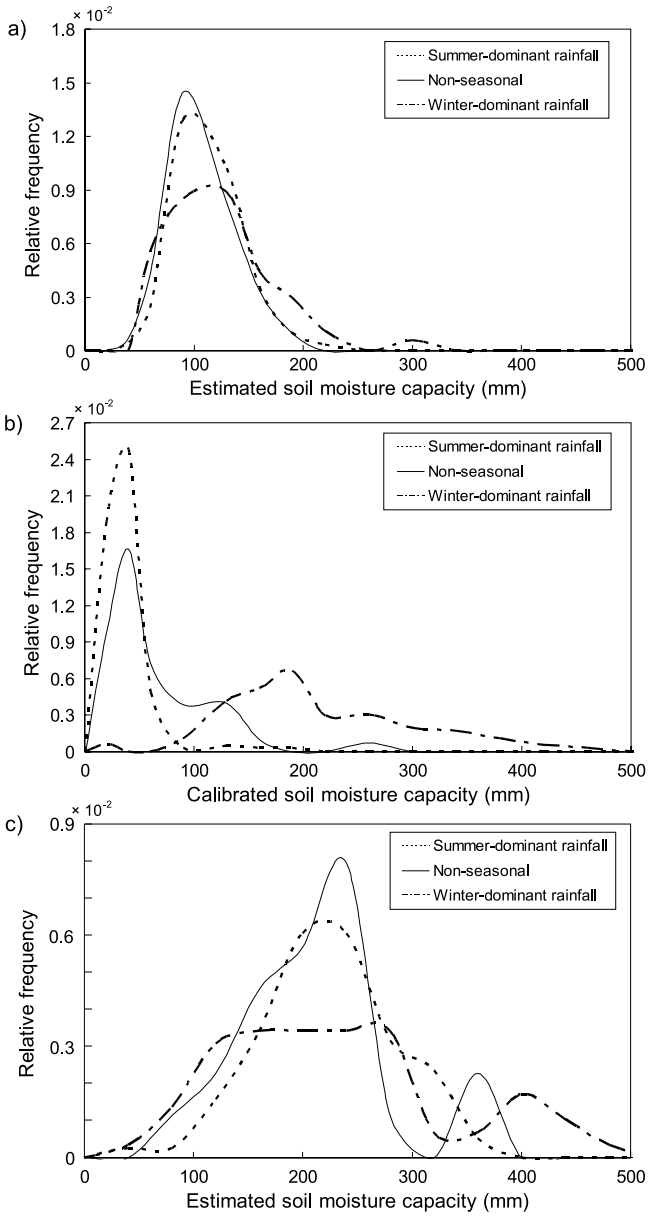

Figure 5. Histogram of catchment-scale soil moisture capacities, (a) estimated using the method of *McKenzie et al.* [2003], (b) the calibrated soil moisture capacities, and (c) independently estimated empirical values from *Ladson et al.* [2004], grouped by seasonality categories.

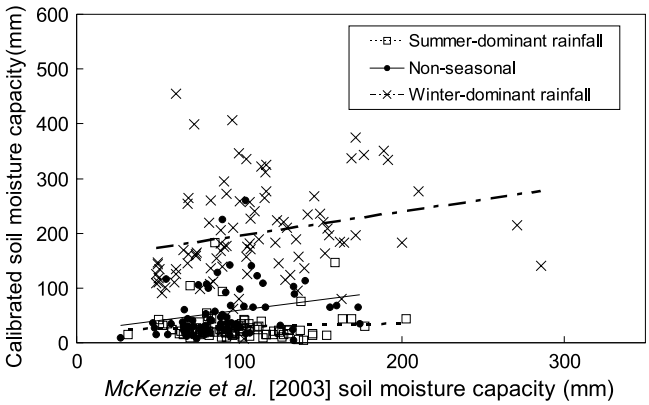

Figure 6. Plot of calibrated soil moisture capacities versus estimated soil moisture capacities using the method of *McKenzie et al.* [2003]. The lines are regressions for each seasonality category. The coefficients of these regressions are given in Table 6.

and some of the nonseasonal rainfall catchments thus had extremely low calibrated soil moisture capacities. The average calibrated soil moisture capacity for summer-dominant rainfall catchments seems too low to be physically reasonable.

[54] Infiltration-excess runoff is not considered in the current model. However, the quantitative effect of this process on water balance could be reproduced by setting the catchment-scale soil moisture capacity to a much smaller value than the actual plant available soil moisture capacity. Similarly to a catchment with infiltration-excess runoff as the main runoff process, a catchment with an excessively small soil moisture capacity would produce runoff from a storm regardless of the antecedent moisture conditions. Of course, from a modeling perspective, this situation is not desirable. The point here is that we would expect the s_{max} parameter to be significantly underestimated by calibration of this model in catchments where infiltration-excess runoff is the primary runoff production process.

[55] In contrast, the calibrated soil moisture capacities are much larger than the *McKenzie et al.* [2003] estimates for winter-dominant catchments. One possible reason for this could be a significant underprediction by *McKenzie et al.* [2003] of the soil moisture capacities for heavily forested catchments. To explore this idea, we examined the relationship between the calibrated soil moisture capacities and a measure of the percentage of the catchment covered with forest. Figure 7 shows a plot of the calibrated soil moisture capacities against independently estimated forest cover for each catchment. The slope of the regression is significant at the 95% level, although many catchments have small calibrated soil moisture capacities that seem unrelated to the percentage forest cover variable. Nevertheless, there is an upward trend in the data, and many of the highest calibrated soil moisture capacities are associated with dense forest cover, especially in the winter-dominant rainfall catchments.

Table 6. Coefficients of Regression of Calibrated Soil Moisture Capacities Against the Capacities From *McKenzie et al.* [2003]

	R^2	Slope	Slope 95% Confidence Interval	Intercept	Intercept 95% Confidence Interval
All	0.09	0.74	(0.45, 1.04)	20	(−11, 52)
Summer	0.01	0.06	(−0.10, 0.22)	23	(6, 39)
Nonseasonal	0.12	0.47	(0.17, 0.77)	13	(−16, 43)
Winter	0.06	0.44	(0.06, 0.81)	150	(105, 196)

5.2. Comparison With *Ladson et al.*'s [2004] Soil Moisture Capacities

[56] As noted in section 2.1.2, the soil moisture capacities derived by *Ladson et al.* [2004] (Figure 5b) are not directly comparable with the estimated and calibrated values (also in Figure 5b) because the catchments are not the same. However, they are useful in analyzing whether a systematic seasonality difference is present in the soil moisture capacity values. The *McKenzie et al.* [2003] soil moisture capacity estimates cover much the same region as the estimates used in the *Ladson et al.* [2004] study.

[57] *Ladson et al.* [2004, p. 17] state that "estimates of available water capacity from *McKenzie et al.* [2000] [an earlier Australia-wide soil moisture capacity estimation] could be considered a reasonable lower bound on field-based estimates of the actual dynamic soil moisture store." Comparison between Figures 5a and 5c indicates that the soil moisture capacities from *McKenzie et al.* [2003] are systematically lower than those of *Ladson et al.* [2004].

[58] Nevertheless, consistent with the data of McKenzie et al., no systematic difference in capacities across seasonality categories is apparent in the *Ladson et al.* [2004] data. This result reinforces the observation in the previous section that the calibrated capacities in the summer-dominant rainfall catchments may be spurious, further strengthening the proposition that infiltration-excess runoff may be predominant in these catchments. On the other hand, the distribution of capacity from *Ladson et al.* [2004] is broadly consistent with calibrated values for winter-dominant rainfall catchments.

5.3. Possible Reasons for Lack of Fit

[59] We identified several potential reasons why the mean annual evapotranspiration predictions of the seasonal model might overpredict the observed values for summer-dominant rainfall catchments and/or underpredict for winter-dominant rainfall catchments with the estimated

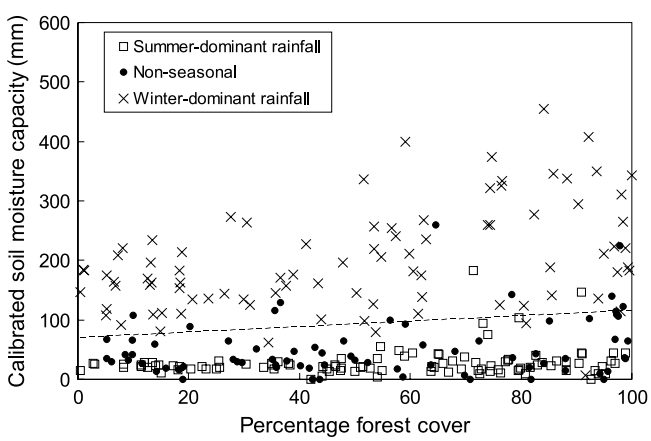

Figure 7. Plot of percentage forest cover versus calibrated soil moisture capacities. The dashed line is the regression line for all of the catchments.

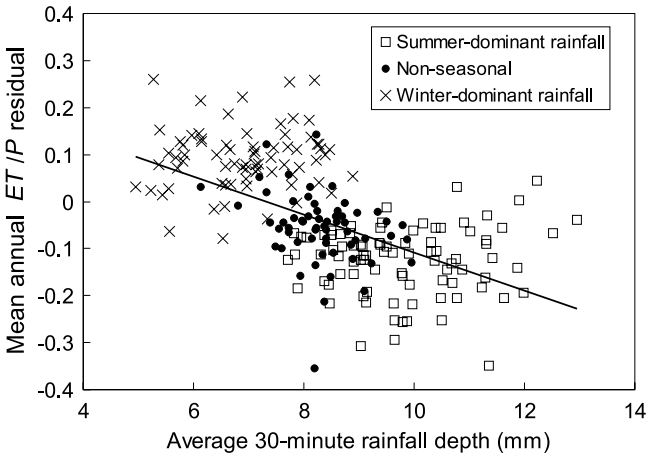

Figure 8. Estimated average rainfall intensity against mean annual evapotranspiration residuals (observed minus predicted).

catchment-scale soil moisture capacities. In light of the previously reported literature that suggests that simple models based on supply and demand of hydrological inputs can adequately model mean annual water balance, the data presented here suggest that additional model components may be required, or that errors may be present in the data. We systematically analyzed these possibilities. However, most of these possibilities could be ruled out.

[60] 1. The model does not simulate infiltration-excess runoff. *Milly* [1994b, 2143–2144] notes that "two related characteristics of land surfaces, finite water storage capacity and finite permeability, may be identified as possible causes of such additional runoff." We suggest that especially for some of the summer dominant rainfall catchments in this study, the finite permeability of soil may be the primary runoff generation process. The low calibrated soil moisture capacities for some of the summer-dominant rainfall catchments as plotted in Figures 5 and 6 supports this idea. The model might be fitting infiltration-excess runoff data by forcing the soil moisture capacity to assume unreasonably low values. Also, a comparison of the average rainfall intensity estimates [*Lu et al.*, 2003] against the residual evapotranspiration ratio (Figure 8) provides further evidence for our hypothesis. There is a clear relationship between the rainfall seasonality and the average rainfall intensities, with summer-dominant rainfall catchments having greater average intensities (this is also shown in Table 1). Moreover, a regression of the residuals against the rainfall intensities was found to be statistically significant. Infiltration-excess runoff is also dependent on the permeability of the soil in the catchment; we were, however, unable to find any relationship between the residuals and the soil permeabilities, nor was there a relationship between the permeabilities and the rainfall seasonality.

[61] 2. We expected that a ramp actual evapotranspiration function [e.g., *Rodriguez-Iturbe et al.*, 1999] might yield more accurate model predictions. As noted in section 2.3.2, *Milly* [2001] showed that the use of a step function rather than a ramp function gave approximately equal values of mean annual evapotranspiration ratios, but the difference was largest under arid conditions. Because many of the catchments studied here are arid (in terms of the dryness index $\overline{E_p}/\overline{P}$), we considered the possibility that the use of ramp functions might improve our predictions. However, we found that the predictions of evapotranspiration were more accurate in arid catchments than in humid catchments. Thus we saw no reason to use the more complicated description of evapotranspiration.

[62] 3. We also considered what effect errors in assumed potential evapotranspiration values might have on the results. We used the estimated areal potential evapotranspiration values from the *Bureau of Meteorology* [2001] and obtained similar results to using the values from *Raupach et al.* [2001a]. Also, we considered whether underpredicted potential evapotranspiration values were responsible for the poor fit of the winter-dominant evapotranspiration predictions. We found that only by doubling the Priestley-Taylor estimates was it possible to reconcile the predicted evapotranspiration values with the observed values. We judged this to be unrealistic.

[63] 4. Finally, we considered whether the rainfall data might be systematically biased across the seasonality categories. *Milly and Dunne* [2002] suggest that high-elevation locations tend to be underrepresented in rainfall gauge networks. Furthermore, these higher-elevation locations tend to have higher average rainfall than the rest of the catchment because of orographic effects. As a result, the average rainfall in catchments with high maximum altitudes relative to the average altitude may have a systematic bias in the estimated basin mean annual rainfall. Therefore we examined the distribution of average and maximum altitudes across the different seasonality categories. We found no systematic relation between potential orographic sampling error of rainfall and catchment seasonality categories. We conclude that this orographic bias did not explain the seasonality-related structure of model errors. However, a sensitivity analysis indicated that the seasonal difference between the observed evapotranspiration ratios (Figure 1a and Table 3) could be made statistically insignificant by introducing a seasonally dependent rainfall bias of around 5–10%. Rainfall gauge and sampling biases of this order of magnitude are not uncommon, and the presence of seasonally dependent rainfall biases may partially explain the discrepancy between the observed data and the predicted results. However, we were unable to identify a systematic rainfall bias with the present data. Furthermore, rainfall biases by themselves on the order of 5–10% are unable to describe the total difference between the observed and predicted evapotranspiration ratios.

6. Conclusions

[64] A stochastic soil moisture accounting model with seasonally varying forcing, based on the model presented by *Milly* [1994b], was used to estimate mean annual evapotranspiration for a number of Australian catchments. It was assumed in the model that rainfall arrivals were Poisson distributed, with a time-dependent arrival rate. Storm depths were modeled as an exponential distribution. The arrival rate, storm depth parameter, and the potential evapotranspiration rate were all modeled as cosine curves with annual periods and arbitrary phase shifts. Runoff occurring by gravity drainage of the root zone was explicitly modeled, whereas infiltration-excess runoff was not. The catchments were categorized as having summer-dominant, winter-

dominant or nonseasonal rainfall regimes. The soil moisture capacity of each basin was estimated from an earlier independent analysis.

[65] The expected value of mean annual evapotranspiration was computed for each catchment by running a Monte Carlo simulation. The resulting predictions were compared with the observed mean annual evapotranspiration and with estimates of mean annual evapotranspiration as a simple function of the dryness index of the catchment. We concluded that for a given value of the dryness index, the observed mean annual evapotranspiration for summer-dominant catchments was lower than for winter-dominant catchments. The predictions had the opposite results.

[66] We also determined for each catchment the values of soil moisture capacity for which the predicted mean annual evapotranspiration would be equal to the observed evapotranspiration. The calibrated soil moisture capacity for most summer-dominant rainfall catchments was significantly lower than the estimated [*McKenzie et al.*, 2003] values, indicating that infiltration-excess runoff may be hydrologically important in these catchments. Furthermore, the evapotranspiration ratio residuals were shown to be significantly related to the average rainfall intensity estimates of *Lu et al.* [2003]. The calibrated values of soil moisture capacity for winter-dominant rainfall catchments were, in general, much higher than the estimated [*McKenzie et al.*, 2003] values but were still physically reasonable. The calibrated soil moisture capacities for nonseasonal catchments were weakly related to the estimated [*McKenzie et al.*, 2003] values.

[67] Of course, infiltration-excess runoff is much more likely to occur in summer-dominant rainfall catchments. This conclusion of this study should not be interpreted as affirming this well-known observation; rather, this paper concludes that explicit modeling of infiltration-excess runoff may be needed to explain the mean annual water balance of Australian catchments, which is often safely disregarded in other mean annual water balance studies. The most obvious direction for further research is incorporation of infiltration-excess runoff into the model in order to more accurately model mean annual evapotranspiration for the Australian catchments considered here.

[68] **Acknowledgments.** This study was supported by the Cooperative Research Centre for Catchment Hydrology under Project 2.3, "Predicting the effects of land-use changes on catchment water yield and stream salinity," and the Murray-Darling Basin Commission funded project "Integrated assessment of the effects of land use changes on water yield and salt loads" (D2013). Financial support for the corresponding author was provided by the Cooperative Research Centre for Catchment Hydrology in the form of a postgraduate scholarship. We would like to thank Andrew Western, Francis Chiew, Murray Peel, John Gallant, Hua Lu for providing the data used in this study. We would also like to thank Andrew Western, Barry Croke, and five anonymous reviewers for their very helpful suggestions on ways to improve the paper.

References

Atkinson, S. E., R. A. Woods, and M. Sivapalan (2002), Climate and landscape controls on water balance model complexity over changing timescales, *Water Resour. Res.*, *38*(12), 1314, doi:10.1029/2002WR001487.

Budyko, M. I. (1974), *Climate and Life*, Elsevier, New York.

Bureau of Meteorology (2001), *Climatic Atlas of Australia*, set 3, *Evapotranspiration*, Aust. Gov. Publ. Serv., Canberra, ACT.

Farmer, D., M. Sivapalan, and C. Jothityangkoon (2003), Climate, soil, and vegetation controls upon the variability of water balance in temperate and semiarid landscapes: Downward approach to water balance analysis, *Water Resour. Res.*, *39*(2), 1035, doi:10.1029/2001WR000328.

Ladson, T., J. Lander, A. Western, and R. Grayson (2004), Estimating extractable soil moisture content for Australian soils, *Tech. Rep. 04/3*, Coop. Res. Cent. for Catchment Hydrol., Clayton, Vic., Australia.

Laio, F., A. Porporato, L. Ridolfi, and I. Rodriguez-Iturbe (2001), Plants in water-controlled ecosystems: Active role in hydrologic processes and response to water stress II. Probabilistic soil moisture dynamics, *Adv. Water Resour.*, *24*, 707–723.

Lu, H., C. J. Moran, I. P. Prosser, M. R. Raupach, J. Olley, and C. Petheram (2003), Sheet and rill erosion and sediment delivery to streams: A basin wide estimation at hillslope to medium catchment scale, *Tech. Rep. 15/03*, CSIRO Land and Water, Canberra, ACT, Australia.

McKenzie, N. J., D. W. Jacquier, L. J. Ashton, and H. P. Creswell (2000), Estimation of soil properties using the atlas of Australian soils, *Tech. Rep. 11/00*, CSIRO Land and Water, Canberra, ACT, Australia.

McKenzie, N. J., J. C. Gallant, and L. J. Gregory (2003), Estimating water storage capacities in soil at catchment scales, *Tech. Rep. 03/3*, Coop. Res. Cent. for Catchment Hydrol., Clayton, Vic., Australia.

Milly, P. C. D. (1993), An analytic solution of the stochastic storage problem applicable to soil water, *Water Resour. Res.*, *29*, 3755–3758.

Milly, P. C. D. (1994a), Climate, interseasonal storage of soil water, and the annual water balance, *Adv. Water Resour.*, *17*, 19–24.

Milly, P. C. D. (1994b), Climate, soil water storage, and the average annual water balance, *Water Resour. Res.*, *30*, 2143–2156.

Milly, P. C. D. (2001), A minimalist probabilistic description of root zone soil water, *Water Resour. Res.*, *37*, 457–463.

Milly, P. C. D., and K. A. Dunne (2002), Macroscale water fluxes: 1. Quantifying errors in the estimation of basin mean precipitation, *Water Resour. Res.*, *38*(10), 1205, doi:10.1029/2001WR000759.

Peel, M. C., F. H. S. Chiew, A. W. Western, and T. A. McMahon (2000), Extension of unimpaired monthly streamflow data and regionalisation of parameter values to estimate streamflow in ungauged catchments, report, Natl. Land and Water Resour. Audit, Canberra, ACT, Australia. (Available at http://audit.ea.gov.au/anra/water/docs/national/Water_Streamflow.htm)

Priestley, C. H. B., and R. J. Taylor (1972), On the assessment of the surface heat flux and evaporation using large-scale parameters, *Mon. Weather Rev.*, *100*, 81–92.

Raupach, M. R., J. M. Kirby, D. J. Barrett, and P. R. Briggs (2001a), Balances of water, carbon, nitrogen and phosphorus in Australian landscapes: (1) Project description and results, *Tech. Rep. 40/01*, CSIRO Land and Water, Canberra, ACT, Australia.

Raupach, M. R., J. M. Kirby, D. J. Barrett, P. R. Briggs, H. Lu, and L. Zhang (2001b), Balances of water, carbon, nitrogen and phosphorus in Australian landscapes: (2) Model formulation and testing, *Tech. Rep. 41/01*, CSIRO Land and Water, Canberra, ACT, Australia.

Rodriguez-Iturbe, I., V. K. Gupta, and E. Waymire (1984), Scale considerations in the modeling of temporal rainfall, *Water Resour. Res.*, *20*, 1611–1619.

Rodriguez-Iturbe, I., A. Porporato, L. Ridolfi, V. Isham, and D. R. Cox (1999), Probabilistic modelling of water balance at a point: The role of climate, soil and vegetation, *Proc. R. Soc. London, Ser. A*, *455*, 3789–3805.

Sankarasubramanian, A., and R. M. Vogel (2002), Annual hydroclimatology of the United States, *Water Resour. Res.*, *38*(6), 1083, doi:10.1029/2001WR000619.

Wolock, D. M., and G. J. McCabe (1999), Explaining spatial variability in mean annual runoff in the conterminous United States, *Clim. Res.*, *11*, 149–159.

Woods, R. (2003), The relative roles of climate, soil, vegetation and topography in determining seasonal and long-term catchment dynamics, *Adv. Water Resour.*, *26*, 295–309.

Zhang, L., W. R. Dawes, and G. R. Walker (2001), Response of mean annual evapotranspiration to vegetation changes at catchment scale, *Water Resour. Res.*, *37*, 701–708.

Zhang, L., K. Hickel, W. R. Dawes, F. H. S. Chiew, A. W. Western, and P. R. Briggs (2004), A rational function approach for estimating mean annual evapotranspiration, *Water Resour. Res.*, *40*, W02502, doi:10.1029/2003WR002710.

A. J. Jakeman, Integrated Catchment Assessment and Management Centre, Australian National University, Canberra, ACT 0200, Australia.

T. A. McMahon, Department of Civil and Environmental Engineering, University of Melbourne, Melbourne, Vic 3010, Australia.

P. C. D. Milly, U.S. Geological Survey, Princeton, NJ 08542, USA.

N. J. Potter and L. Zhang, CSIRO Land and Water, Canberra, ACT 2601, Australia. (nicholas.potter@csiro.au)